Preparation and characterization of octadecane/polyurea nanocapsule-embedded poly(ethylene oxide) nanofibers

ARTICLE *in* JOURNAL OF APPLIED POLYMER SCIENCE · JUNE 2015

Impact Factor: 1.77 · DOI: 10.1002/app.42539

5 AUTHORS, INCLUDING:

Won-Gun Koh

Yonsei University

72 PUBLICATIONS **1,610** CITATIONS

SEE PROFILE

In Woo Cheong

Kyungpook National University

131 PUBLICATIONS **1,210** CITATIONS

SEE PROFILE

Jung Hyun Kim

Hanbat National University

210 PUBLICATIONS **2,175** CITATIONS

SEE PROFILE

Journal of Applied Polymer Science

Preparation and characterization of octadecane/polyurea nanocapsule-embedded poly(ethylene oxide) nanofibers

Jun-Won Kook,[1] Wonseok Cho,[1] Won-Gun Koh,[1] In Woo Cheong,[2] Jung Hyun Kim[1]

[1]Department of Chemical and Biomolecular Engineering, Yonsei University, Seodaemoon-Gu, Seoul 120-749, Republic of Korea
[2]Department of Applied Chemistry, Kyungpook National University, Buk-gu, Daegu 702-701, Republic of Korea
Correspondence to: J. Kim (E-mail: jayhkim@yonsei.ac.kr)

ABSTRACT: This article describes the preparation and characterization of latent heat storage poly(ethylene oxide) nanofibers (LHS-PEO nanofibers) with octadecane/polyurea (PCM/PU) nanocapsules. PCM/PU nanocapsules were prepared by interfacial polycondensation from toluene 2,4-diisocyanate and ethylene diamine in a resin-fortified emulsion system. LHS-PEO nanofibers were prepared using an electrospinning procedure with varying PCM/PU nanocapsules content, i.e., from 0 to 8 wt %. The PCM/PU nanocapsules were polydisperse with an average diameter of 200 nm. The melting and freezing temperatures were determined as 23.7 and 28.2°C, respectively, and the corresponding latent heats were determined as 123.4 and 124.1 kJ kg^{-1}, respectively. The encapsulation efficiency of the PCM/PU nanocapsules was 78.1%. The latent heat capacity of the LHS-PEO nanofibers increased as the PCM/PU nanocapsules content increased. Defects, such as holes and disconnection of the nanofibers, were observed, particularly inside the LHS-PEO nanofibers. For packaging applications, mats were fabricated from the nanocapsules-embedded nanofibers with varying nanocapsule content and the mats' surface temperatures were monitored with a thermal imaging camera. The results proved the feasibility of using the LHS-PEO nanofibers for thermal energy storage and functional packaging materials. © 2015 Wiley Periodicals, Inc. J. Appl. Polym. Sci. **2015**, *132*, 42539.

KEYWORDS: electrospinning; nanostructured polymers; phase behavior; synthesis and processing; thermal properties

Received 3 February 2015; accepted 26 May 2015
DOI: 10.1002/app.42539

INTRODUCTION

A phase-change material (PCM) is a substance that changes phase between gas, liquid, and solid without changing temperature, while absorbing or releasing a large amount of energy called "latent heat".[1] A representative organic-type PCM is paraffin. Various melting–freezing temperatures and large latent heats of paraffin are evaluated for utilization as a PCM in practical applications.

To allow for practical applications, embedment or encapsulation of PCM is required because of the fluidity or deformability of PCM around the phase transition temperature.[2–11]

One other method for embedding PCM is its direct injection into the polymer nanofiber by using coaxial electrospinning. When PCM is loaded directly into the polymer nanofiber, it is difficult to control the nanofiber morphology and physical properties.[12–21]

In our previous studies, to improve the stability of polymer nanofiber with PCM, we used PCM nanocapsules made by miniemulsion polymerization or interfacial polycondensation processes. However, surfactants used in our previous process act to bring out impurities, causing mechanical instability and changes in particle morphology. Therefore, it is required to remove the residual surfactant.[22–24]

In this study, to solve this problem, we synthesized nanosized PCM/polyurea (PCM/PU) capsules by interfacial polycondensation with poly(4-styrenesulfonic acid-co-maleic acid) sodium salt (PSSMA) as a reactive surfactant. The PSSMA react with NCO bond and NH_2 bond in the raw materials for polyurea during the interfacial polycondensation. Therefore, the reactive surfactant, PSSMA, is remained on the PCM/PU capsules after condensation process.

Furthermore, to verify the performance of PCM/PU nanocapsules, we prepared latent heat storage poly(ethylene oxide) nanofibers with various PCM/PU nanocapsule contents. However, to our knowledge, there have been few reports about poly(ethylene oxide) nanofibers with embedded PCM/PU nanocapsules manufactured by electrospinning.

We analyzed morphology, phase-change behavior, thermal properties, and thermal behavior of the latent heat storage poly(ethylene oxide) nanofibers.

EXPERIMENTAL

Materials

Toluene 2, 4-diisocyanate (TDI), octadecane, poly(4-styrenesulfonic acid-co-maleic acid) sodium salt (PSSMA, $M_n = 20{,}000$ g mol^{-1}), and poly(ethylene oxide) (PEO, $M_n = 600{,}000$ g mol^{-1}) were purchased from Aldrich (MA, USA). Ethylene diamine (EDA) was obtained from Samchun Pure Chemicals (S. Korea). An electrospinning device equipped with a high-voltage supply, a syringe pump (KDS100; KD scientific, USA), a stainless-steel nozzle, and an 18 G syringe needle was purchased from NanoNC (NNC-ESP60, S. Korea). All chemicals were used as received without further purification. Deionized (DI) water was used in all the experiments.

Preparation of PCM/PU Nanocapsules

The PCM/PU nanocapsules were prepared in a 300 mL double-jacketed glass reactor equipped with a mechanical stirrer and three inlets. First, 0.6 g of PSSMA was dissolved in 80 g of DI water. Nine grams of octadecane (PCM) was added to the PSSMA aqueous solution, and the solution was emulsified using a homogenizer (T25 basic ULTRA-TURAX, IKA, Germany) at 50°C and 9000–10,000 rpm for 10 min. After homogenization, the mixture was added into the reactor and stirred for 5 min at 600 rpm. Second, 8.1 g of EDA aqueous solution (3.1 g EDA + 5.0 g DI water) was slowly added into the reactor. The reaction was maintained for 5 h at 65°C.

Preparation of LHS-PEO Nanofibers

Scheme 1 shows schematic process using the PCM/PU-PEO solution by electrospinning method. LHS-PEO nanofibers were prepared from PEO and the PCM/PU nanocapsule emulsion with a varying PCM/PU nanocapsules content of 2, 6, and 8 wt %. The predetermined amount of PEO was dissolved in the PCM/PU emulsion with the fixed concentration at 5 wt %. The PEO solution containing the PCM/PU nanocapsules was injected into a silicone tube with an 18 G syringe needle through a syringe pump at a flow rate of 0.18 mL h^{-1}. Approximately, 10–11 kV was maintained with a high-voltage supply. The spinning distance was 10 cm.

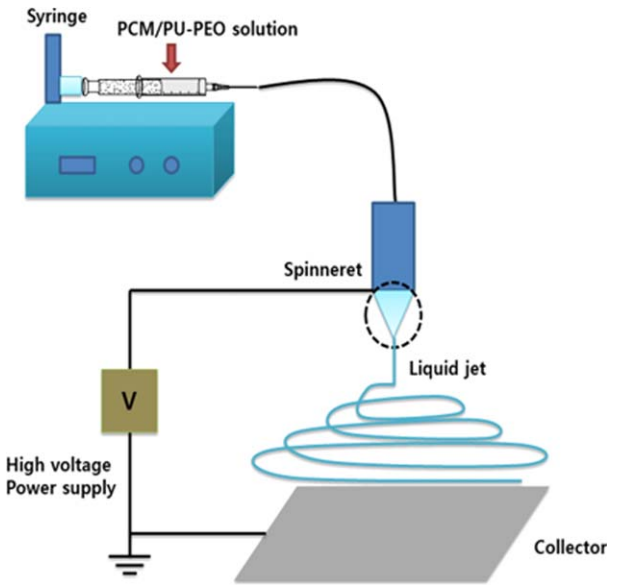

Scheme 1. Schematic of the electrospinning process using the PCM/PU-PEO solution. [Color figure can be viewed in the online issue, which is available at wileyonlinelibrary.com.]

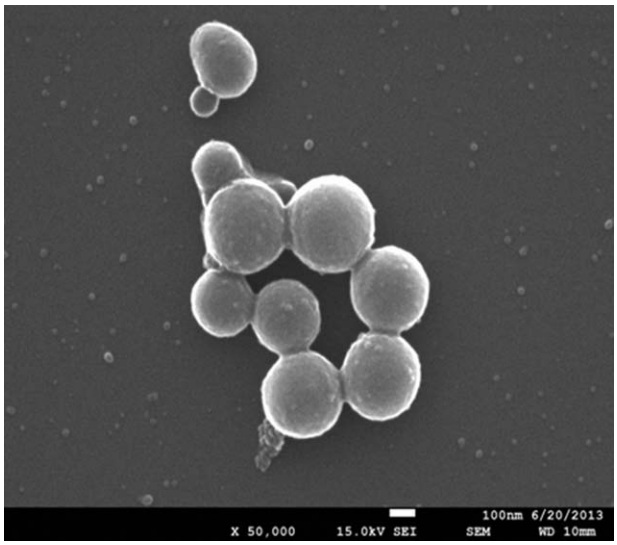

Figure 1. SEM image of PCM/PU nanocapsules.

Morphological Analysis

The PCM/PU nanocapsule morphology and LHS-PEO nanofiber were observed by field-emission scanning electron microscopy (FE-SEM; JSM 7001F, JEOL, Japan) and transmission electron microscopy (TEM; JSM 100CXII, UHR, JEOL, Japan). The samples for FE-SEM and TEM analyses were prepared by directly mounting as-spun nanofibers onto a silicon wafer and copper grids, respectively.

Thermal Analysis

The latent heat capacity of the LHS-PEO nanofibers was measured by differential scanning calorimetry (DSC, DSC Q10, TA instrument, USA). The heating and cooling ranges were 0–60°C at a rate of 10°C min^{-1}. Thermal properties of LHS-PEO

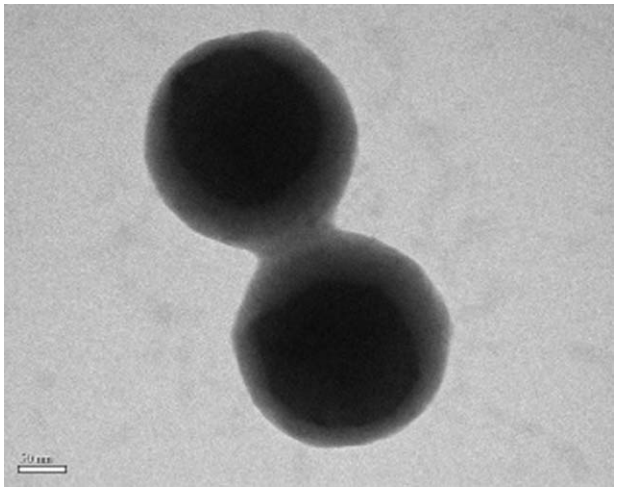

Figure 2. TEM image of PCM/PU nanocapsules.

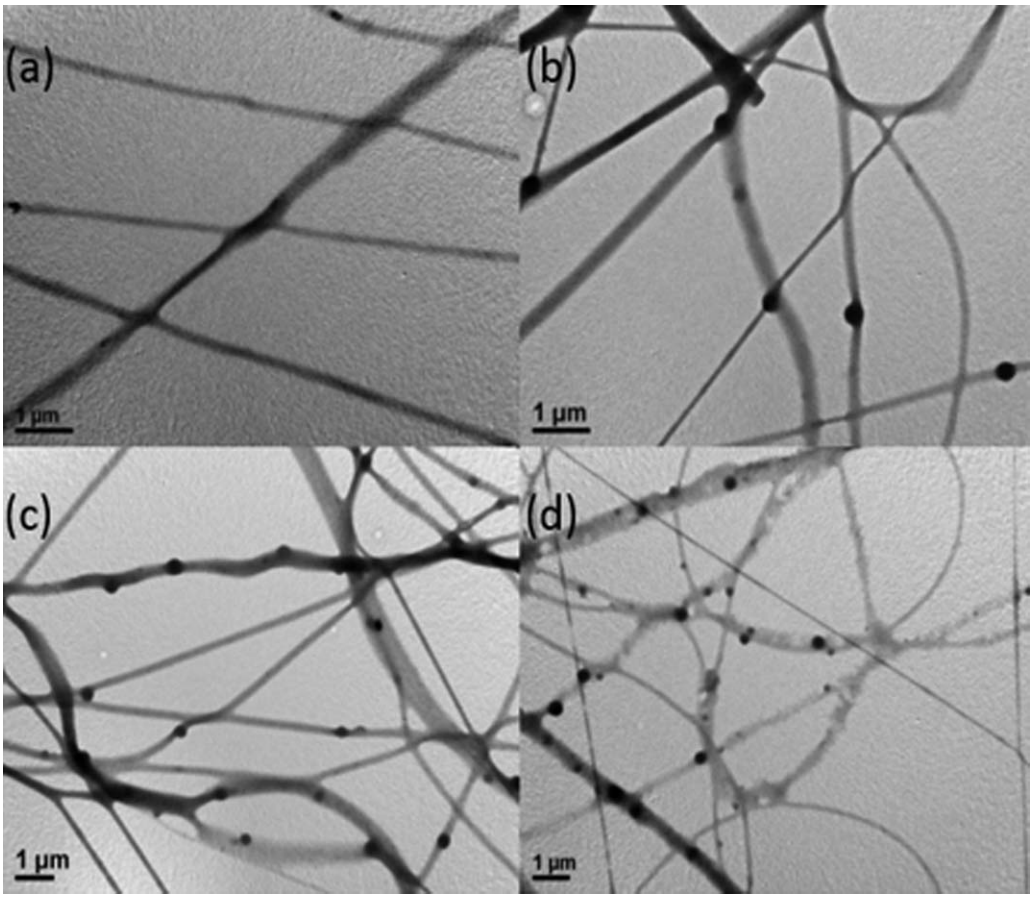

Figure 3. TEM images of LHS-PEO nanofibers prepared with varying PCM/PU nanocapsule content: (a) pristine PEO nanofiber, (b) 2 wt %, (c) 6 wt %, and (d) 8 wt %.

nanofibers were measured by thermogravimetric analysis (TGA, TGA Q50, TA instrument, USA) under an N_2 atmosphere. The heating range was from 30 to 600°C at a rate of 10°C min^{-1}.

Thermal Image Camera Measurements

A thermal imaging camera (R300SR, Nippon Electric Company, Japan) was used to film in 3 s intervals. The size of LHS-PEO nanofiber mat was 2 × 2 × 0.1 cm. The mat was mounted on a hot plate at 30°C.

RESULTS AND DISCUSSION

Synthesis of PCM/PU Nanocapsules

PCM/PU nanocapsules were synthesized by interfacial polycondensation in a resin-fortified emulsion. The formation mechanisms of PCM/PU nanocapsules have been described in previous work.[23] TDI monomer, which forms a single phase with PCM (octadecane), mostly localizes at the interface between the PCM droplets and the aqueous phase. Shell formation is achieved by the urea-bond formation reaction between water-soluble EDA and oil-soluble TDI at the PCM–droplet interface. PCM/PU nanocapsules morphology was observed by the SEM and TEM, as shown in Figures 1 and 2. The PCM/PU core/shell nanocapsules were polydisperse with an average diameter of 200 nm. The PCM/PU nanocapsules latent heats of melting and crystallization were determined to be 123.4 and 124.1 kJ kg^{-1}, respectively.

Morphology of LHS-PEO Nanofibers

Figure 3 shows the TEM images of pristine PEO nanofibers and LHS-PEO nanofibers with varying PCM/PU nanocapsules

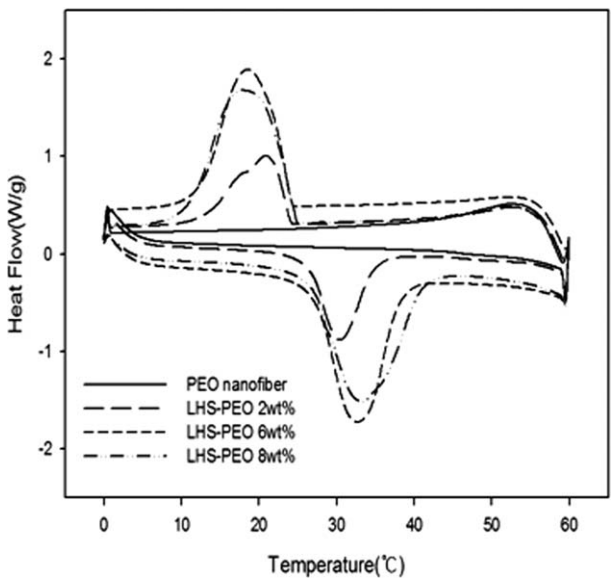

Figure 4. DSC curve of pristine PEO and LHS-PEO nanofibers with varying PCM/PU nanocapsule content.

Table I. Phase Transition Temperature and Corresponding Latent Heats of Pristine PEO Nanofibers and PCM/PU Nanocapsule-Embedded LHS-PEO Nanofibers

Nanofibers	T_m (°C)	T_f (°C)	ΔT (°C)	H_m (J/g)	H_f (J/g)
Pristine	–	–	–	–	–
LHS-PEO 2 wt %	30.41 (±0.27)	20.89 (±0.21)	9.51 (±0.48)	27.84	26.61
LHS-PEO 6 wt %	32.71 (±0.59)	18.51 (±0.37)	14.19 (±0.96)	59.26	73.12
LHS-PEO 8 wt %	33.08 (±0.70)	18.89 (±0.48)	14.19 (±1.18)	63.63	76.69

content. This figure shows the pristine PEO nanofibers with the average thickness of 180 nm. When the PCM/PU nanocapsules content was increased to 2, 6, and 8 wt %, the number of PCM/PU nanocapsules embedded in the PEO nanofiber increased. The surface of the LHS-PEO nanofibers was uneven and irregular due to the embedment of PCM/PU nanocapsules. As the PCM/PU nanocapsules content increased to 8 wt %, the LHS-PEO nanofibers were not successfully prepared as before. Defects, such as holes and disconnection around the LHS-PEO nanofibers, could be seen, as shown in Figure 3.

Nanofiber mat prepared by the electrospinning process has a high latent heat capacity due to the improvement of the stability of PCM in the polymer nanofiber by using PU capsulation technique. So, it has better performance of heat capacity than other polymer-based PCM.

Phase-Change Behavior of LHS-PEO Nanofibers

As shown in Figure 4, the phase-change enthalpies of pristine PEO nanofibers and LHS-PEO nanofibers by using different PCM/PU nanocapsule content were recorded. The onset temperatures of melting and freezing transitions for heating and cooling cycles, respectively, were about 27°C, which is the typical phase-transition temperature of octadecane. Phase-transition temperature of the PCM is changed as the chain length of carbon structure. However, the latent heat capacity of octadecane is not changed in melting and solidification because there is no chemical reaction between PCM molecules in melting and freezing cycles. The melting, freezing temperature (T_m, T_f) and the melting, freezing latent heat (ΔH_m, ΔH_f) of the LHS-PEO nanofibers were also obtained from DSC analysis, as shown in Table I. All embedded PCM/PU nanocapsules in the LHS-PEO nanofibers had a higher T_m and a lower T_f. Furthermore, the differences between the melting and freezing temperatures of LHS-PEO nanofibers shown in Table I indicate that the degree of supercooling of the PCM/PU nanocapsules decreased as the amount of embedded PCM/PU nanocapsules in the LHS-PEO nanofiber increased. PCM/PU nanocapsules had higher T_m and lower T_f than octadecane. Because polyurea shell and PEO nanofiber matrix with lower thermal conductivity acted as additional heat transfer barrier. Therefore, when the content of PCM/PU nanocapsule is gradually increased, the supercooling of PCM/PU nanocapsule was decreased. (Thermal conductivity of octadecane = 0.22 W $m^{-1}\cdot K^{-1}$, thermal conductivity of polyurea = 0.17 W $m^{-1}\cdot K^{-1}$, and thermal conductivity of PEO = 0.17 W $m^{-1}\cdot K^{-1}$.)

Table II. Mass Ratio between PEO and PCM/PU Nanocapsule

Nanofibers	PEO : PCM/PU capsule (wt)
Pristine	–
LHS-PEO 2 wt %	1 : 0.38
LHS-PEO 6 wt %	1 : 1.14
LHS-PEO 8 wt %	1 : 1.52

Pristine PEO nanofibers showed no transition peaks (the solid line in Figure 4). For the nanofibers with the nanocapsules, melting and freezing transition peaks were clearly observed (the dashed lines in Figure 4). As the nanocapsule content increased, the peak height or area for the transitions also increased.

Table II shows the mass ratio of PCM/PU nanocapsules to nanofiber. In the mass ratio, the portion of PCM/PU nanocapsules gradually increased. Due to the increase in the number of PCM/PU nanocapsules per unit volume, the stability of the pristine PEO nanofibers decreased.

Thermal Properties of LHS-PEO Nanofibers

The thermal properties of LHS-PEO nanofibers were evaluated by TGA and thermal imaging analysis. Figure 5 shows the TGA curves for LHS-PEO nanofibers prepared by varying the PCM/PU nanoparticle content. The thermal decomposition temperature of the PCM is about 140–150°C. Polyurea and PEO have thermal decomposition temperatures at 240–260°C and 400°C, respectively.

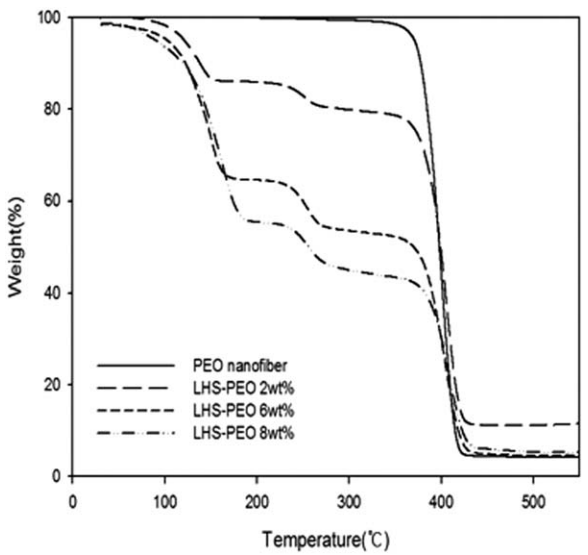

Figure 5. TGA curve of LHS-PEO nanofibers with varying PCM/PU nanocapsule content.

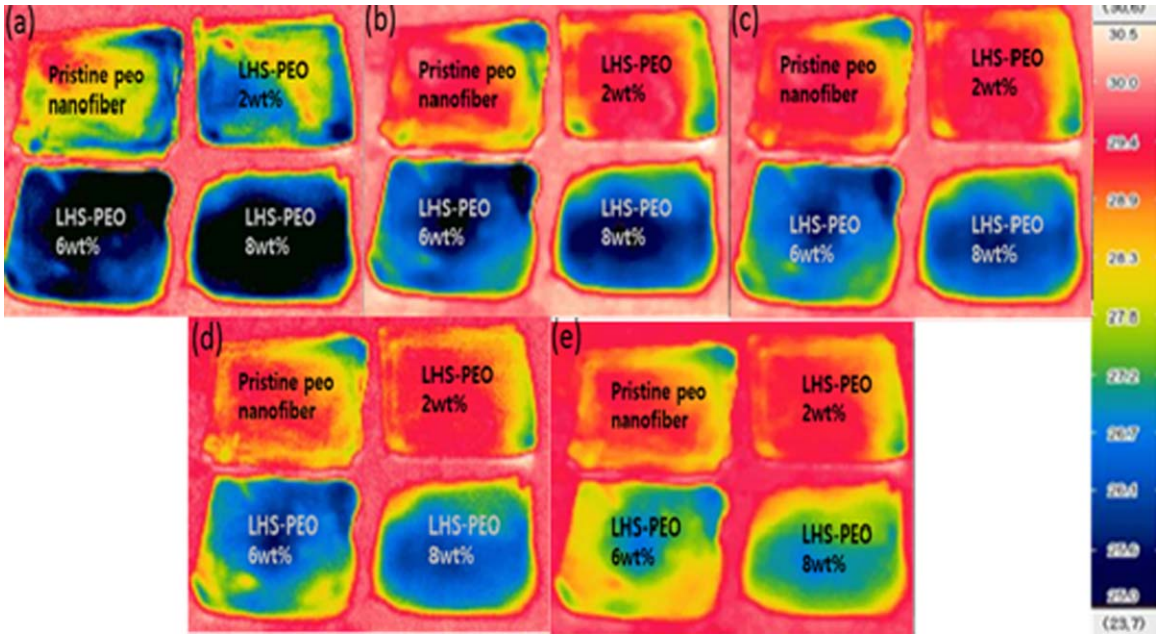

Figure 6. Thermal behavior of LHS-PEO nanofiber mats with varying PCM/PU nanocapsule content using a thermal imaging camera: (a) 0 s, (b) 15 s, (c) 30 s, (d) 60 s, and (e) 180 s. [Color figure can be viewed in the online issue, which is available at wileyonlinelibrary.com.]

Figure 6 shows the thermal behavior of LHS-PEO nanofibers with varying PCM/PU nanocapsule content. As shown, the temperature change of pristine PEO nanofiber and LHS-PEO 2 wt % nanofiber mats were started from 15 s. On the contrary, the temperature change of others were slower than pristine PEO nanofiber and LES-PEO 2 wt %, which can be attributed to the latent heat increase as the PCM/PU nanocapsule content was increased from 2 to 8 wt %.

As shown in Table I, the latent heat capacities of LHS-PEO nanofiber as various PCM/PU nanocapsule content were analyzed quantitatively. By measuring the weight of LHS-PEO nanofiber mat, the latent heat of LHS-PEO nanofiber mat can be calculated. Therefore, we found out that the thermal behavior of various LHS-PEO nanofibers was closed to our prediction. We just quantitatively explained thermal behavior of LHS-PEO nanofiber by TGA measurement shown in Figure 5 and data in Table I. So, the prediction value was slightly different from the actual value. In this article, by the increase of PCM/PU nanocapsule content, the thermal behavior of LHS-PEO nanofiber mat showed the expected trend.

CONCLUSION

We successfully prepared LHS-PEO nanofibers with embedded PCM/PU nanocapsules by electrospinning. The melting/freezing latent heat increased with an increase in the PCM/PU nanocapsule content. However, defects, such as holes and disconnection around the LHS-PEO 8 wt %, were confirmed in TEM images. The reason for these defects is that as the PCM/PU nanocapsule content increases, the amount of PEO per unit area of nanofiber decreases, and as such, the stability of the LHS-PEO nanofiber decreases. The melting and freezing temperatures of the LHS-PEO nanofiber were determined as 23.7 and 28.2°C, respectively, and the maximum latent heat of the LHS-PEO nanofiber was determined as 76.69 J g^{-1}. The thermal behavior of LHS-PEO nanofiber with varying PCM/PU nanocapsules content was filmed with a thermal imaging camera. The results showed that the LHS-PEO nanofiber mats reached a specific temperature at different speeds, because the number of embedded PCM/PU nanocapsule in the PEO nanofiber per unit volume is different from the solid content of embedded PCM/PU nanocapsule content in the PEO nanofiber. The proposed LHS-PEO nanofiber can be used in various applications (e.g., thermal energy storage and functional packaging materials) associated with PCM.

ACKNOWLEDGMENTS

This research was supported by the Pioneer Research Center Program through the National Research Foundation of Korea (NRF) funded by the Ministry of Science, ICT & Future Planning (2010–0019550) and by Ministry of Trade Industry and Energy/Korea Evaluation Institute of Industrial Technology (KEIT) (10043265). And the Nano Material Technology Development Program through the National Research Foundation of Korea (NRF) funded by the Ministry of Education, Science and Technology (2008–2002380/2012–0006227). This research was also supported by the Converging Center Program through the Ministry of Education, Science and Technology (2010K001430).

REFERENCES

1. Hittle, D. C.; Andre, T. L. *ASHRAE Trans.* **2002**, *108*, 175.
2. Cho, J.-S.; Kwon, A.; Cho, C.-G. *Colloid Polym. Sci.* **2002**, *280*, 260.
3. Torini, L.; Argillier, J.; Zydowicz, N. *Macromolecules* **2005**, *38*, 3225.
4. Siddhan, P.; Jassal, M.; Agrawal, A. K. *J. Appl. Polym. Sci.* **2007**, *106*, 786.

5. Lu, S.; Xing, J.; Zhang, Z.; Jia, G. *J. Appl. Polym. Sci.* **2011**, *121*, 3377.
6. Lu, S.-f.; Xing, J.-w.; Zhang, Z.-h.; Jia, G.-p. *Polym. Mater. Sci. Eng.* **2010**, *12*, 014.
7. Zhang, H.; Sun, S.; Wang, X.; Wu, D. *Colloids Surf. A* **2011**, *389*, 104.
8. Spernath, L.; Magdassi, S. *Polym. Adv. Technol.* **2011**, *22*, 2469.
9. Rosenbauer, E.-M.; Landfester, K.; Musyanovych, A. *Langmuir* **2009**, *25*, 12084.
10. Hong, K.; Park, S. *Mater. Sci. Eng. A* **1999**, *272*, 418.
11. Kong, X. Z.; Jiang, W.; Jiang, X.; Zhu, X. *Polym. Chem.* **2013**, *4*, 5776.
12. Sanchez-Silva, L.; Tsavalas, J.; Sundberg, D.; Sánchez, P.; Rodriguez, J. F. *Ind. Eng. Chem. Res.* **2010**, *49*, 12204.
13. Sun, D. H.; Xu, T. Y.; Liu, Y. J.; Zhang, M. *Adv. Mater. Res.* **2011**, *306*, 37.
14. McCann, J. T.; Marquez, M.; Xia, Y. *Nano Lett.* **2006**, *6*, 2868.
15. Hu, W.; Yu, X. *RSC Adv.* **2012**, *2*, 5580.
16. Chen, C.; Wang, L.; Huang, Y. *Mater. Lett.* **2009**, *63*, 569.
17. Nagamine, S.; Kosaka, K.; Tohyama, S.; Ohshima, M. *Mater. Res. Bull.* **2014**, *50*, 108.
18. Tran, C.; Kalra, V. *J. Power Sources* **2013**, *235*, 289.
19. Alay, S.; Göde, F.; Alkan, C. *Fibers Polym.* **2010**, *11*, 1089.
20. Arecchi, A.; Mannino, S.; Weiss, J. *J. Food Sci.* **2010**, *75*, N80.
21. Crespy, D.; Friedemann, K.; Popa, A. M. *Macromol. Rapid Commun.* **2012**, *33*, 1978.
22. Crespy, D.; Stark, M.; Hoffmann-Richter, C.; Ziener, U.; Landfester, K. *Macromolecules* **2007**, *40*, 3122.
23. Kwon, H. J.; Cheong, I. W.; Kim, J. H. *Macromol. Res.* **2010**, *18*, 923.
24. Park, S.; Lee, Y.; Kim, Y. S.; Lee, H. M.; Kim, J. H.; Cheong, I. W.; Koh, W.-G. *Colloids Surf. A* **2014**, *450*, 46.